

Thickness and temperature dependence of electrical properties of Bi₂(Te_{0.1}Se_{0.9})₃ thin films

V. Damodara Das and S. Selvaraj

Citation: *Journal of Applied Physics* **86**, 1518 (1999); doi: 10.1063/1.370923

View online: <http://dx.doi.org/10.1063/1.370923>

View Table of Contents: <http://scitation.aip.org/content/aip/journal/jap/86/3?ver=pdfcov>

Published by the [AIP Publishing](#)

Articles you may be interested in

Temperature-dependent structural property and power factor of n type thermoelectric Bi_{0.90}Sb_{0.10} and Bi_{0.86}Sb_{0.14} alloys

Appl. Phys. Lett. **103**, 242108 (2013); 10.1063/1.4844635

Assembly of one-dimensional nanorods into Bi₂S₃ films with enhanced thermoelectric transport properties

Appl. Phys. Lett. **90**, 112106 (2007); 10.1063/1.2712504

Size-dependent optical properties of sputter-deposited nanocrystalline p-type transparent CuAlO₂ thin films

J. Appl. Phys. **97**, 084308 (2005); 10.1063/1.1866485

Preparation and characterization of p-type Sb₂Te₃ and n-type Bi₂Te₃ thin films grown by coevaporation

J. Vac. Sci. Technol. A **19**, 899 (2001); 10.1116/1.1354600

Size and temperature dependence of electrical resistance and thermoelectric power of Bi₂Te₂Se₁ thin films

J. Appl. Phys. **83**, 3696 (1998); 10.1063/1.366594



Thickness and temperature dependence of electrical properties of $\text{Bi}_2(\text{Te}_{0.1}\text{Se}_{0.9})_3$ thin films

V. Damodara Das^{a)} and S. Selvaraj

Thin Film Laboratory, Department of Physics, Indian Institute of Technology, Madras, Chennai 600 036, India

(Received 22 September 1998; accepted for publication 13 April 1999)

Thin films of different thicknesses have been vacuum deposited onto clean glass plates held at room temperature using the flash evaporation technique in a vacuum of 2×10^{-5} Torr. The structural characterization of the bulk and the thin films was carried out using x-ray diffraction, transmission electron microscopy, and selected area electron diffraction techniques. Electrical resistance and thermoelectric power of the films were measured in the same vacuum of 2×10^{-5} Torr in the temperature range 300–450 K. The conduction activation energy of the films was calculated using the electrical resistivity and thermoelectric power data of the films. The thickness dependence of the activation energy observed is attributed to the polycrystalline nature of the films. Grain growth and reorientation of the grains take place during the annealing process. The thickness dependence of electrical resistivity and thermoelectric power of the films are explained by the effective mean free path model [C. R. Tellier, *Thin Solid Films* **51**, 311 (1978)]. The important physical parameters like mean free path, Fermi energy, power index of the energy dependant expression for the mean free path, the hypothetical bulk resistivity and the thermoelectric power have been calculated by the combined analysis of electrical resistivity and thermoelectric power. The electron-phonon scattering mechanism is found to be dominant in the material. © 1999 American Institute of Physics. [S0021-8979(99)05214-7]

I. INTRODUCTION

Semiconducting thermoelements find applications in thermoelectric devices like power generators, refrigerators, IR devices, etc. Currently, Bi_2Te_3 , PbTe and Si-Ge alloys are found to be the most important thermoelectric materials. Bi_2Te_3 semiconductors exhibit a higher thermoelectric figure of merit than the other two semiconductors. Solid solutions of Bi_2Te_3 and Bi_2Se_3 are found to enhance the thermoelectric figure of merit further above that of the Bi_2Te_3 material due to the reduced thermal conductivity.¹ There have been a number of works on thermoelectric power, electrical resistivity, Hall coefficient, etc. of Bi_2Te_3 - Bi_2Se_3 semiconductors in the bulk state.²⁻¹⁴ However, there is not much work in the thin film state on these materials. In this article, we report the size effect analysis of thermoelectric power and electrical resistivity of Bi_2Te_3 - Bi_2Se_3 ternary alloy thin films of a particular composition $x=0.9$ among $\text{Bi}_2(\text{Te}_{1-x}\text{Se}_x)_3$ solid solutions. Thickness and grain size are related nearly linearly with each other. Hence, the dependence of various properties on the thickness and the grain size are similar.

II. EXPERIMENT

A bulk alloy of $\text{Bi}_2(\text{Te}_{0.1}\text{Se}_{0.9})_3$ semiconductor was prepared by melting the required amounts of elements in an evacuated (2×10^{-5} Torr) quartz ampoule by heating it in a muffle furnace. The system was kept at the melting points of each of the elements for one day. Then, the temperature was

increased to just above the melting point of the alloy system and was maintained at that temperature for two days. The quartz ampoule was shaken frequently during this period to ensure thorough mixing. After this, the temperature was reduced to just below the melting point of the alloy system and the alloy system was annealed at this temperature for four days. Finally, the temperature was gradually decreased to room temperature.

The bulk alloy thus obtained was powdered into tiny particles and was used as charge for preparing the thin films, using the flash evaporation technique. The powdered particles were taken in a basket, attached to which there was a hollow cylindrical tube. Just below the bottom end of this tube was a rectangular tantalum boat which was connected to two electrodes for heating it. The basket was vibrated using a relay switch due to which the particles (charge), guided through the hollow cylindrical tube, would fall onto the hot boat which was maintained at a temperature much above the boiling point of the alloy. This led to an instantaneous evaporation of the alloy particles. The vibration of the basket was controlled by adjusting the voltage supplied to the relay switch, and hence, the deposition rate was also controlled to the same value (15 \AA/s) for all films. Films were grown at room temperature onto ultrasonically cleaned glass plates. Thickness and deposition rate were monitored using the quartz crystal monitor.

Thin films were structurally characterized using x-ray diffraction (XRD), transmission electron microscopy (TEM) and selected area electron diffraction (SAD) techniques. Electrical resistance was measured in vacuum as a function of temperature in the temperature range 300–450 K. Thermal

^{a)}Electronic mail: vddas@acer.iitm.ernet.in

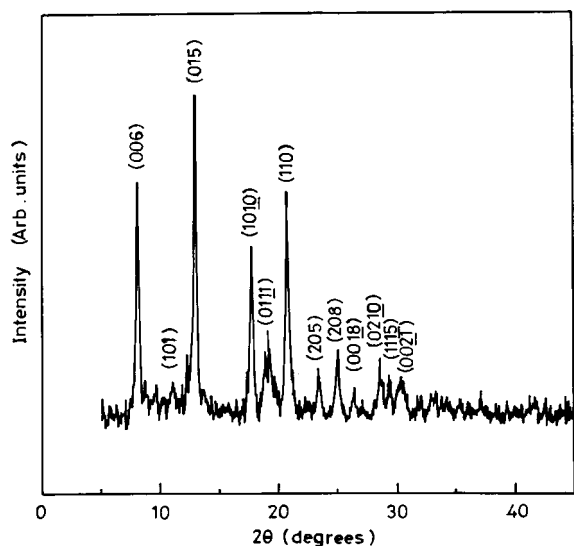


FIG. 1. XRD pattern of the bulk alloy. Radiation used; $\text{MoK}\alpha_1$, $\lambda = 0.709 \text{ \AA}$.

emf across the thin films was also measured in the temperature range of 300–450 K in vacuum using the integral technique using copper as the other material of the thermocouple. Large area copper pad pressure contacts were used for the measurement of electrical resistance and thermal emf of the films. Copper–Constantan thermocouples were used for the temperature measurement. Electrical resistance value of the films for our studies are found to be of the order of a few kilohms (above 2 k Ω), whereas the contact resistance value is found to be tens of milli ohms, which is too small compared to the electrical resistance of the films. Electrical resistance was also measured using tin contacts (precoated before deposition of the films). It was found that the film resistance measured using the tin contacts agreed well with that measured using copper pad contacts. We have used large

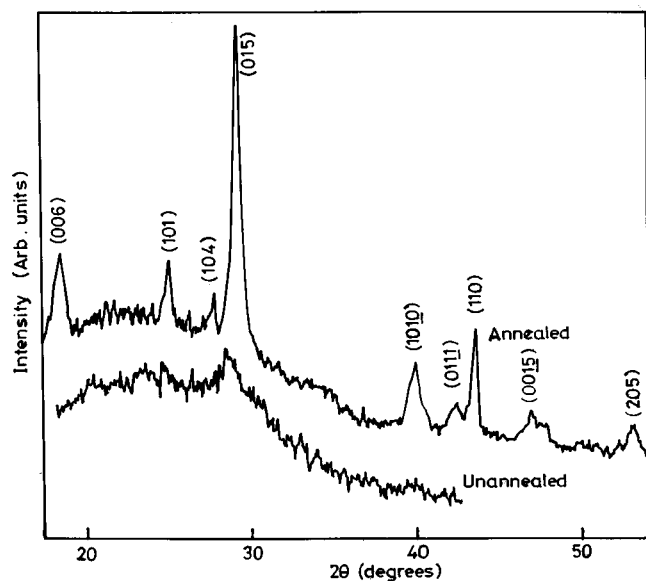


FIG. 2. XRD patterns of typical annealed and unannealed thin film of thickness 1800 Å. Radiation used: $\text{CuK}\alpha_1$; $\lambda = 1.541 \text{ \AA}$.

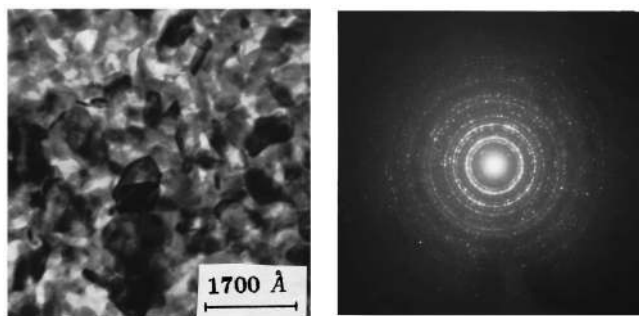


FIG. 3. Transmission electron micrograph (TEM) and selected area electron diffraction (SAD) pattern of a thin film.

area ($>1 \text{ cm}^2$) copper pad contacts to ensure that there is a perfect very low resistance, ohmic electrical contact. The contact resistance is of the order of few tens of a milliohms.

III. RESULTS AND DISCUSSION

XRD patterns shown in Figs. 1 and 2 for the bulk alloy and the thin film, respectively, reveal their polycrystalline nature. The larger number of sharp peaks observed for the annealed film compared to the unannealed film indicates that grain growth and grain reorientation take place during the annealing program. Electron micrograph (TEM) and electron diffraction (SAD) patterns shown in Fig. 3 also confirm the XRD observation. The d values obtained using all these techniques agree with the American Standard for Testing and Materials (ASTM) d values of Bi_2Te_3 and Bi_2Se_3 compounds. This confirms the alloy formation in both the bulk and thin film states. Grain size, calculated for annealed films using the XRD patterns, indicates that it increases as the film thickness increases (Table I). It is seen from Fig. 2 that the unannealed film shows a weak and broad (015) peak. This indicates that the crystallite size is small. However, the annealed film shows a sharp (015) peak due to grain growth during annealing. Since, we observe weak peaks for the unannealed film, grain size calculation is less accurate for these compared to that for the annealed films. However, we have given the approximate grain size values for unannealed films in Table I. We have used annealed films for our electrical investigations.

IV. TEMPERATURE DEPENDENCE OF ELECTRICAL RESISTIVITY AND THERMOELECTRIC POWER

A. Electrical resistivity

Resistivity of the films was calculated from the measured resistance values using the dimensions of the films.

TABLE I. Variation of grain size with thickness.

Thickness (Å)	Grain size (Å)	
	As-grown	Annealed
1000	150	180
1400	160	200
1800	180	230

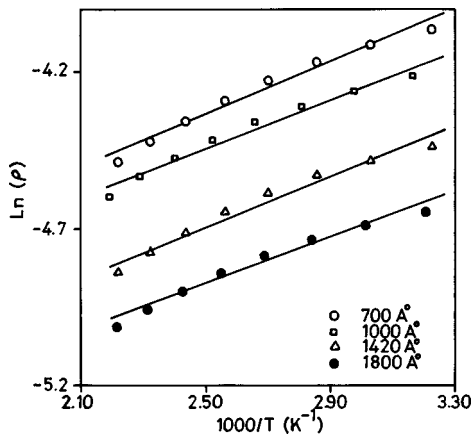


FIG. 4. Plot of $\ln(\rho)$ vs $1000/T$ for thin films of different thicknesses.

Conduction activation energy values (ΔE) of the films calculated from the Arrhenius plots of resistivity (Fig. 4) indicate that the activation energy for conduction decreases as the film thickness increases. This is attributed to the polycrystalline nature of the films in which the grain boundary potential decreases as the grain size increases.¹⁵⁻¹⁷

B. Thermoelectric power

Thermoelectric power measurement in the temperature range 300–450 K indicated the n -type nature of the films. The temperature dependence of the thermoelectric power of semiconductors is given by the expression,¹⁸

$$S = -\frac{k}{e} \left[\frac{E(0)}{kT} - \frac{\gamma}{k} + A \right], \quad (1)$$

where $E(0)$ is the activation energy, k and e the usual physical constants, γ the temperature coefficient of activation energy for conduction and A is a constant which depends on the nature of scattering. Normally, A is a constant between 2 and 4. Activation energy values $E(0)$ were obtained from the slopes of the plots of thermoelectric power versus reciprocal temperature (Fig. 5). The γ values have been obtained from the linear plots of the Peltier coefficient Π ($=ST$) as a function of temperature¹⁹ and A values have been obtained from

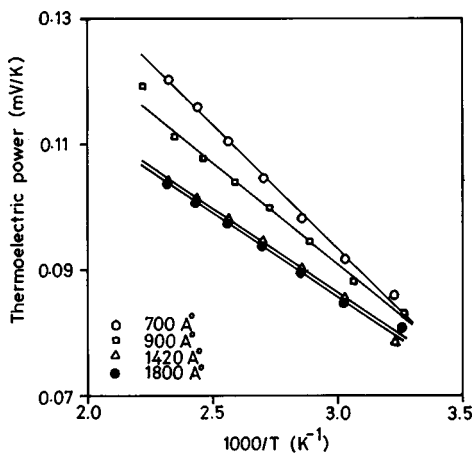


FIG. 5. Thermoelectric power variation as a function of reciprocal temperature for films of different thicknesses.

TABLE II. Activation energy values ΔE and $E(0)$, γ and A .

Thickness (Å)	Activation energy (meV)		γE (eV K ⁻¹)	A
	ΔE	$E(0)$		
700	40	40	3.0×10^{-4}	3.7
1000	30	35	2.7×10^{-4}	3.4
1400	35	30	2.6×10^{-4}	3.2
1800	30	30	2.6×10^{-4}	3.2

the above expression. The results are given in Table II. Activation energy values ΔE and $E(0)$, obtained respectively from the Arrhenius plots of resistivity and the plots of thermoelectric power versus reciprocal temperature, closely agree with each other. This indicates that electrical conduction takes place mainly in the conduction band (above E_C) and there is no hopping conduction in the films.¹⁸ Activation energy value decreases as the film thickness increases, which is as is expected. Value of A close to 3 is attributed to lattice scattering in a material.¹ We have also found the A values to be around 3, and hence, predominant scattering in this material film is lattice scattering. However, there is a slight deviation of our A values from 3 which could be due to small scattering contributions from other scattering processes and the experimental inaccuracies.

V. THICKNESS DEPENDENCE OF ELECTRICAL RESISTIVITY AND THERMOELECTRIC POWER

A. Electrical resistivity

When the thickness of a material is comparable to a length characteristic of the given phenomenon, classical or quantum size effect occurs. Classical size effect occurs when at least one of the charge carrier motion parameters having the dimension of length becomes of the order of the film thickness. Thus, when the mean free path of the charge carrier is comparable to the thickness of a material, the important transport properties such as electrical resistivity and thermoelectric power are affected. Size effect on electrical resistivity has been analyzed over many years by various workers. Fuchs–Sondheimer²⁰ model accounted well the size effect on electrical resistivity of single crystalline thin films. However, their model was not suitable to explain electrical resistivity of polycrystalline thin films. So, Mayadas, and Shatzkes²¹ developed a new model to account for the grain boundary scattering in polycrystalline thin films. But, this model was too complicated and it was difficult for analysis. Tellier²² developed a simple effective mean free path model for polycrystalline thin films. According to this model, resistivity (ρ_f) of a polycrystalline thin film is given by

$$\rho_f = \rho_g \left[1 + \frac{3}{8t} (1-p) l_g \right], \quad (2)$$

where ρ_g is the “grain boundary” resistivity, i.e., resistivity of the hypothetical bulk which has the same microstructure as that of the film, p the specularity parameter, l_g the effective mean free path in the above hypothetical bulk and t the thickness of the film.

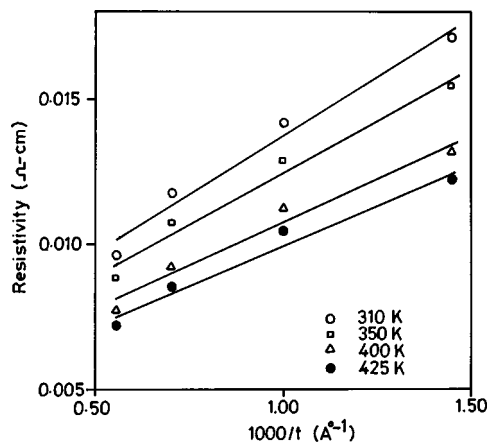


FIG. 6. Electrical resistivity as a function of reciprocal thickness at different temperatures.

According to this equation, a plot of resistivity versus reciprocal thickness is a straight line. The slope gives the value of $(3/8)(1-p)l_g$ and the intercept gives the value of ρ_g . ρ_g is called the hypothetical bulk resistivity because, it is the resistivity of a film, having the same microstructure as that of the films prepared, whose thickness is infinity (i.e., $1/t=0$). Figure 6 shows the plots of resistivity values as a function of reciprocal thickness at different temperatures. From the slopes of the linear plots, we have calculated the mean free path values l_g at different temperatures assuming $p=0$ for our polycrystalline films. Values of l_g and ρ_g are given in Table III. The mean free path value decrease as the temperature increases due to increased lattice vibrations.

B. Thermoelectric power

Pichard *et al.*²³ extended the effective mean free path model of Tellier, developed for electrical resistivity, to calculate the thermoelectric power of thin films. Thermoelectric power of thin films in the effective mean free path model is given by

$$S_f = S_g \left[1 - \frac{3}{8t} (1-p) l_g \frac{U_g}{1+U_g} \right], \quad (3)$$

where

$$S_g = \frac{\pi^2 k^2 T}{3eE_F} (1+U_g) \quad \text{and} \quad U_g = \left(\frac{\partial \ln l_g}{\partial E} \right)_{E_F}$$

S_g is known as the thermoelectric power of the infinitely thick film or the bulk having the same microstructure as that of the films.

TABLE III. Physical parameters obtained using size effect analysis.

Temperature (K)	$\rho_g \times 10^{-3}$ (Ω cm)	S_g (μ V/K)	l_g (\AA)	U_g	E_F (eV)	$n \times 10^{19}$ (cm^{-3})
310	5.7	75.0	3800	-0.070	0.094	7.4
350	5.3	83.7	3600	-0.083	0.094	7.5
400	4.8	88.7	3300	-0.131	0.096	8.0
425	4.5	91.3	3200	-0.143	0.097	8.2

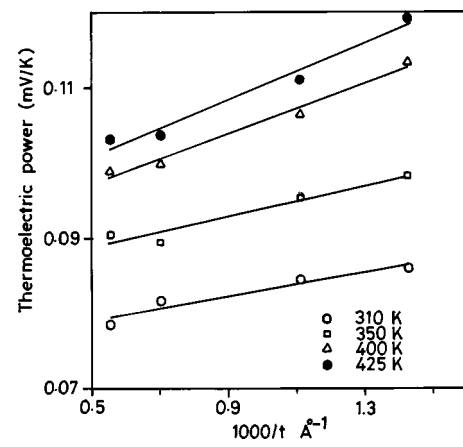


FIG. 7. Thermoelectric power as a function of reciprocal thickness at different temperatures.

From this equation, we can obtain the slope as $(3/8) \times [U_g / (1+U_g)] l_g S_g$ assuming $p=0$, from the plots of S_f vs $1/t$ at different temperatures. S_g values can be obtained from the y intercepts of these plots. Figure 7 shows the plots of thermoelectric power of thin films as a function of reciprocal thickness. U_g values are determined using the l_g values obtained from the size effect analysis of electrical resistivity of the films. The negative values of U_g indicate that the mean free path decreases with the increase in energy of the electrons. Mean free path variation with energy depends on the scattering mechanism. For the electron-phonon scattering interaction, mean free path decreases with the increase in energy, whereas, for ionic and ionized impurities types of scattering interaction, mean free path increases with the increase in energy.¹ This alloy system is a ternary compound semiconductor in which all types of scattering mechanisms can be operating simultaneously. But, the negative value of U_g indicates that the electron - phonon scattering interaction is the dominant one in this material.

Fermi energy $E(F)$ values were calculated from the S_g values determined from the intercept of the plot of S_f versus reciprocal thickness. Using the calculated Fermi energy values, electron concentration n was evaluated using the formula,

$$n = \frac{4\pi}{\sqrt{\pi}} (2\pi m^* kT/h^2)^{3/2} F_{1/2} \quad (4)$$

where m^* is effective mass of the electrons, k the Boltzmann constant, T the temperature and $F_{1/2}$ the Fermi integral. Reported effective mass value of $m^*/m=0.3$ (Ref. 24) for the composition of $\text{Bi}_2(\text{Te}_{0.1}\text{Se}_{0.9})_3$ has been used for this calculation. Since the Fermi energy value only weakly depends on the temperature, we have used this value of effective mass for all temperatures. It is found that the electron concentration increases with the increases of temperature.

Figure 8 shows the variation of thermoelectric power factor ($S^2\sigma$) of thin films with temperature. Thermoelectric power factor values are found to be small compared to those of the bulk alloy of this composition. This is due to the usual high value of resistivity in the films because of very small grains (due to internal surface scattering effects) in the films

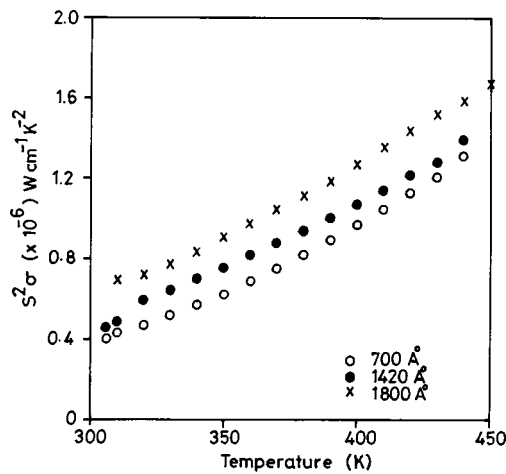


FIG. 8. Variation of thermoelectric power factor ($S^2\sigma$) with temperature for films of different thicknesses.

compared to the bulk value of resistivity, which is much less because of very large size grains (of several micrometers) in the bulk state.

VI. CONCLUSIONS

The bulk and thin films of $\text{Bi}_2(\text{Te}_{0.1}\text{Se}_{0.9})_3$ exhibit a polycrystalline nature. The thickness dependence of the activation energy value is attributed to the grain boundary potential variation with the grain size of the films. The activation energy obtained through resistivity and thermoelectric power data (which agree) indicates that electrical conduction in the films takes place in the conduction band. The sign of thermoelectric power indicates n -type conductivity of the films. The thickness dependence of thermoelectric power and electrical resistivity are explained using the classical size effect theory based on the Tellier's model. Various physical parameters have been calculated using this model. Mean free path decreases with the increase of temperature, as expected. The negative value of the parameter U_g indicates that the electron-phonon interaction is the main scattering mechanism in the material. The Fermi energy value varies slightly with temperature.

ACKNOWLEDGMENTS

The authors are thankful to Mrs. Kanchana Mala, Transmission Electron Microscope Laboratory, Indian Institute of Technology, Madras. One of the authors (S.S) is thankful to IIT, M for financial help rendered during this research work.

- ¹A. F. Ioffe, *Semiconducting Thermoelements and Thermoelectric Cooling* (Infosearch, London, 1957).
- ²H. Wada, M. Watanabe, J. Morimota, and T. Miyakawa, *J. Mater. Res.* **6**, 1711 (1991).
- ³R. G. Cope and A. W. Penn, *J. Mater. Sci.* **3**, 103 (1968).
- ⁴R. Ionescu, J. J. Jaklovsky, N. Nistor, and A. Chiculita, *Phys. Status Solidi A* **27**, 27 (1975).
- ⁵J. Jaklovsky, R. Ionescu, N. Nistor, and A. Chiculita, *Phys. Status Solidi A* **27**, 329 (1975).
- ⁶F. D. Rosi, B. Abeles, and R. V. Jensen, *J. Phys. Chem. Solids* **10**, 191 (1959).
- ⁷H. W. Jeon, H. P. Ha, D. B. Hyun, and J. D. Shim, *J. Phys. Chem. Solids* **52**, 579 (1991).
- ⁸L. Greenaway and G. Harbeke, *J. Phys. Chem. Solids* **26**, 1585 (1965).
- ⁹N. Fuschillo, J. N. Bierly, and F. J. Donohoe, *J. Phys. Chem. Solids* **8**, 430 (1959).
- ¹⁰I. Teramoto and S. Takayanaga, *J. Phys. Chem. Solids* **19**, 124 (1961).
- ¹¹M. V. Vedernikov, V. A. Kutasov, L. N. Luk'yanova, and P. P. Konstantanov, *Proceedings of the 16th International Conference on Thermoelectrics* (IEEE, New Jersey, 1997), pp. 57–62.
- ¹²V. M. Glazov and Yu. V. Yatananov, *Inorg. Mater.* **22**, 30 (1989).
- ¹³G. N. Gordiakaova, G. V. Kokosh, and S. S. Sinani, *Sov. Phys. Tech. Phys.* **3**, 1 (1958).
- ¹⁴C. H. Champness, P. T. Chang, and P. Perekh, *Can. J. Phys.* **43**, 653 (1965).
- ¹⁵V. Damodara Das and S. Selvaraj, *J. Appl. Phys.* **83**, 3696 (1998).
- ¹⁶J. Y. W. Seto, *J. Appl. Phys.* **46**, 5247 (1975).
- ¹⁷J. Dutta, R. Pal, S. K. Battacharya, S. Chaudhuri, and A. K. Pal, *Mater. Chem. Phys.* **36**, 177 (1993).
- ¹⁸N. F. Mott and E. A. Davis, *Electronic Process in Non-Crystalline Materials* (Clarendon, Oxford, 1971), p. 236.
- ¹⁹V. Damodara Das and C. Bahulayan, *Jpn. J. Appl. Phys., Part 1* **34**, 534 (1995).
- ²⁰E. H. Sondheimer, *Adv. Phys.* **1**, 1 (1952).
- ²¹A. F. Mayadas and M. Shatzkes, *Phys. Rev. B* **1**, 1382 (1970).
- ²²C. R. Tellier, *Thin Solid Films* **51**, 311 (1978).
- ²³C. R. Pichard, C. R. Tellier, and A. J. Tossier, *J. Phys. F* **10**, 2009 (1980).
- ²⁴A. F. Ioffe and L. S. Stil'bans, *Rep. Prog. Phys.* **22**, 167 (1959).